Boundary Friction of Aromatic Silane Self-Assembled Monolayers Measured with the Surface Forces Apparatus and Friction Force Microscopy

M. Ruths,*,† N. A. Alcantar,‡ and J. N. Israelachvili‡

Department of Physical Chemistry, Åbo Akademi University, Porthansgatan 3-5, FIN-20500 Åbo, Finland, and Department of Chemical Engineering, University of California, Santa Barbara, California 93106

Received: May 20, 2003; In Final Form: July 29, 2003

The boundary friction of two different aromatic silane monolayers was measured in a single-asperity contact with the surface forces apparatus (SFA) and friction force microscopy (FFM). The measurements were done in ethanol to significantly reduce the adhesion, which allowed a direct, quantitative comparison of load-dependent friction at the molecular level between surfaces of very different radii. A linear dependence of the friction force on load was obtained, and good agreement was found between friction coefficients measured with the two techniques despite the large differences in contact areas, applied loads, and pressures. The friction forces were lower in systems where both contacting surfaces were covered with a monolayer, and chemically bound monolayers were found to better protect the substrates from wear than physisorbed ones.

Introduction

Research on the fundamental aspects of friction has produced a large amount of data on different model systems such as bare crystal surfaces, organic monolayers, and confined liquid films.[1−3] Sometimes the results obtained with different techniques or under only slightly different conditions are conflicting both qualitatively and quantitatively, and it is of general interest to systematically compare data to understand the separate contributions[1] from adhesion and from load in a single-asperity contact. For example, large differences have been observed between the friction measured with the surface forces apparatus (SFA) and friction force microscopy (FFM) on confined polymer melts.[4] This is likely due to differences in the thicknesses of the confined films, because the typical contact areas and range of applied loads in these two techniques give rise to very different pressures in the contact zone.[4] Quantitatively comparable results might be obtainable with these techniques in systems where one or both surfaces are covered with an organic monolayer, chosen so that the thickness and structure of the trapped films (boundary lubricant layers) remain similar within the different pressure ranges investigated.

Variations in friction data obtained with different FFM tips are common, especially in experiments on adhesive systems in vacuum,[2,5] in air of very low humidity,[6] and in ambient air where a microscopic water meniscus gathers around the contact region to cause a strong capillary force.[7,8] At low applied normal loads L, the friction force F in these (adhesive) systems is typically not a linear function of load but is directly proportional to the contact area A given by theories of contact mechanics for adhesive systems (adhesion-controlled friction);[2,5,6] for example, there is a finite friction force even at zero load ($L = 0$). Similar results have been obtained with the SFA for strongly adhesive contacts.[1] On the other hand, in systems with low or no adhesion both FFM[9−11] and SFA[1,12] experiments show a linear increase in friction force with load (load-dependent friction) even at low loads, with the friction force being zero at $L = 0$. Also, in systems that initially show adhesion-dependent friction, the friction becomes a linear function of load at very high loads.[1,12] These experimental observations are generally expressed as[1,12]

$$F = S_c A + \mu L \tag{1}$$

where S_c is the critical shear stress and μ is the friction coefficient. Alternatively, the friction force can be expressed as a shear strength[13] by dividing eq 1 by the contact area A to obtain $S = F/A = S_c + \mu P$, where $P = L/A$ is the pressure.

A description of this type of friction is provided by the so-called "cobblestone model", which is similar to the earlier "Coulomb model" and which proposes that work needs to be done *normally* to the surfaces for them to slide *laterally* past each other.[1,12] This work consists of two quite separate components, the adhesion and the load contributions, which are assumed to be additive. The cobblestone model is in fact an extension to the molecular scale or nanoscale of earlier models of the friction between "interlocking (microscale) asperities", developed for nonadhesive systems,[1,12] where the adhesion enters it as an additional contribution *to the load*.[14] In the cobblestone model, the adhesion contribution scales with the number of bonds involved in the partial separation of the surfaces during sliding, which scales as the contact area A, as indicated in eq 1.[12] The cobblestone model has been used to calculate values for the critical shear stress S_c and the friction coefficient μ that agree rather well with experimental values,[1,12] thus giving the phenomenological expression, eq 1, a physical basis. Because in this model only S_c depends on the interfacial energy γ (the adhesion), it is implied that a reduction in γ would reduce the area-dependence of the friction force, even to the point of removing the area-dependence so that only the term μL remains,[15] which has also been observed experimentally between surfaces that repel each other.[1,12] The cobblestone model thus implies that in systems where there is no adhesion the friction force should increase linearly with the load regardless of the area or how A varies with L and that $F \rightarrow 0$ as $L \rightarrow 0$.

* To whom correspondence should be addressed. Phone: +358-2-2154617. Fax: +358-2-2154706. E-mail: mruths@abo.fi.
† Åbo Akademi University.
‡ University of California.

10.1021/jp0353946 CCC: $25.00
Published on Web 09/17/2003

TABLE 1: Contact Angles and Molecular Areas of Phenyltrichlorosilane (Ph) and Benzyltrichlorosilane (Bz) Monolayers Formed from 0.2% v/v Solution in Anhydrous Toluene on Various Substrates

	Ph monolayer on			Bz monolayer on		
	glass	mica	Si(111)	glass	mica	Si(111)
θ_{adv} (deg)	67 ± 1	44 ± 1	78 ± 1	69 ± 1	70 ± 1	81 ± 1
θ_{rec} (deg)	35 ± 2	19 ± 3	51 ± 1	52 ± 1	60 ± 1	66 ± 3
$\cos \theta_{rec} - \cos \theta_{adv}$	0.43 ± 0.04	0.23 ± 0.03	0.42 ± 0.03	0.26 ± 0.03	0.16 ± 0.03	0.25 ± 0.07
A_{molec} (nm^2)			0.45 ± 0.05			0.27 ± 0.03

The different contributions from the external load and the (internal) adhesion are of interest for understanding friction at the fundamental molecular level. It is also of great practical importance to know under what circumstances the friction between engineering surfaces or measured with probes of different (and perhaps unknown) geometries and radii can be directly compared. This situation is commonly encountered both in practice and in laboratory experiments because the physical or chemical properties of sliding surfaces are often irreversibly modified during prolonged sliding.

We have studied the friction of two aromatic silanes that form chemisorbed (grafted), laterally cross-linked monolayers with different packing density. Aromatic molecules are naturally present in mineral-oil-based lubricants.[16] They are stiffer than alkanes and have more complex lateral interactions in a monolayer, which makes their friction also interesting from a fundamental point of view. Information on the aromatic silane monolayers chosen for our study comes mainly from photopatterning experiments where hydrophilic areas can be formed by irradiation.[17,18] From a practical point of view, silanes form chemically bound self-assembled monolayers (SAMs) on glass substrates which can be used both for SFA and FFM measurements, and the use of grafted monolayers reduces the problem of different film thicknesses seen with confined fluid films. In a parallel FFM investigation,[19] it has been shown that under conditions of low adhesion, the friction of aromatic thiol monolayers is directly proportional to the external load, and tips of different radii R in the range $R = 11-33$ nm give the same friction coefficient. In this study, we extend this comparison to friction measured with SFA and FFM, where the radii of the surfaces differ by 5−6 orders of magnitude.

Materials and Methods

Glass Substrates. The glass substrates used for the SFA and FFM measurements were thin, flexible Pyrex glass bubbles blown from a flame-sealed tube. The preparation of the substrates was a simplification of the method in ref 20 and followed closely the procedure described in ref 21: Small pieces (area ca. 1 cm^2, rms roughness ca. 0.2 nm) were placed on a mica backing sheet, and a 50 nm silver layer was evaporated on their backside. The pieces were glued with their silvered side down onto cylindrical supports for SFA experiments or onto flat magnetic metal disks for FFM measurements using a UV-curing glue, Norland Optical Adhesive no. 61. This glue is prone to plastic deformation at high loads but is sparingly soluble in toluene and ethanol and could be used in the silane self-assembly and friction experiments described below. After the glue was cured with a Pen-Ray lamp (UVP, Upland, CA) for 30 min, the surfaces were rinsed with distilled water and found to be hydrophilic (contact angle <10°). They were dried by blowing with N_2 gas and kept in a N_2 atmosphere for silane deposition or friction experiments.

Silane Monolayers. Phenyltrichlorosilane ($C_6H_5SiCl_3$, hereafter called Ph) and benzyltrichlorosilane ($C_6H_5CH_2SiCl_3$, called Bz), both of purity 97%, were obtained from ABCR GmbH (Karlsruhe, Germany) and used as received. The preparation of 0.2% v/v solutions in anhydrous toluene (Aldrich, 99.8%) and the self-assembly onto different substrates (cf. Table 1) were done in a N_2 atmosphere in a glovebox. The solutions (10−20 mL) were filtered through a flush-cleaned 0.45 μm Acrodisc CR PTFE syringe filter (Gelman Sciences) and used immediately for self-assembly onto one or more of the following: glass surfaces (glued on supports as described above), freshly cleaved mica (2×2 cm^2 squares for atomic force microscopy (AFM) imaging and contact angle measurements and thin back-silvered sheets glued on cylindrical supports), Si(111) wafer pieces (for ellipsometry), and Si tips for FFM (cf. description of tips below and in Table 2). The substrates were withdrawn after 5 min and the remaining drops of trichlorosilane solution blown off with N_2 gas. The samples were then immediately immersed in about 10 mL of anhydrous toluene for 2−3 min, blown dry with N_2, removed from the glovebox, and heated for 10−20 min in an oven at 115−120 °C.

TABLE 2: Properties of the Tips Used for Friction Force Microscopy (FFM)

tip no.	tip chemistry	k_n (N/m)	k_l (N/m)	R (nm)
1	unfunctionalized Si	0.04	4.6	11
2	unfunctionalized Si	0.34	37.8	33
3	Ph on Si	0.05	5.7	16
4	Bz on Si	0.05	5.6	11

Depositions of trichlorosilanes are very sensitive to humidity and other experimental conditions, and with a 1% solution as suggested in ref 18 we obtained an irregular multilayer structure both on glass and on mica, as observed in tapping mode AFM images (Dimension 3000, Digital Instruments). Examples of the AFM height profiles of Ph layers formed at different solution concentrations are shown in Figure 1. At a concentration of 0.1% v/v, the substrate could clearly be recognized between monolayer areas on mica (Figure 1a). The 0.2% v/v concentration selected for this study was found by systematically lowering the solution concentration from 1%. Ph and Bz SAMs formed at 0.2% v/v had a uniform thickness of 0.6−0.9 nm with occasional holes (Figure 1b). Typically, these holes were not as well-defined as the large ones seen in monolayers formed at 0.1% v/v (Figure 1a), and this made the thickness determination more difficult. Figure 1c shows the irregular structure (thicker multilayer patches) obtained at 0.3% v/v.

The advancing and receding contact angles of water on monolayers prepared from 0.2% v/v solution on different substrates are shown in Table 1. Our values are in good agreement with previously reported stationary contact angles of 58−65° for Ph and 64−74° for Bz on glass and Si wafers[17] and advancing contact angles of 63° for Ph and 69° for Bz on fused silica and Si wafers.[18] We find a significantly higher contact angle hysteresis for Ph, about 30°, than for Bz, about 15°.

The thickness of the monolayers on Si(111) was measured at angles of incidence between 40° and 80° with a Beaglehole phase-modulated picometer ellipsometer. The measured thicknesses of 0.5 nm for Ph and 0.8 nm for Bz were used to calculate the molecular area A_{molec} in Table 1, assuming complete cross-

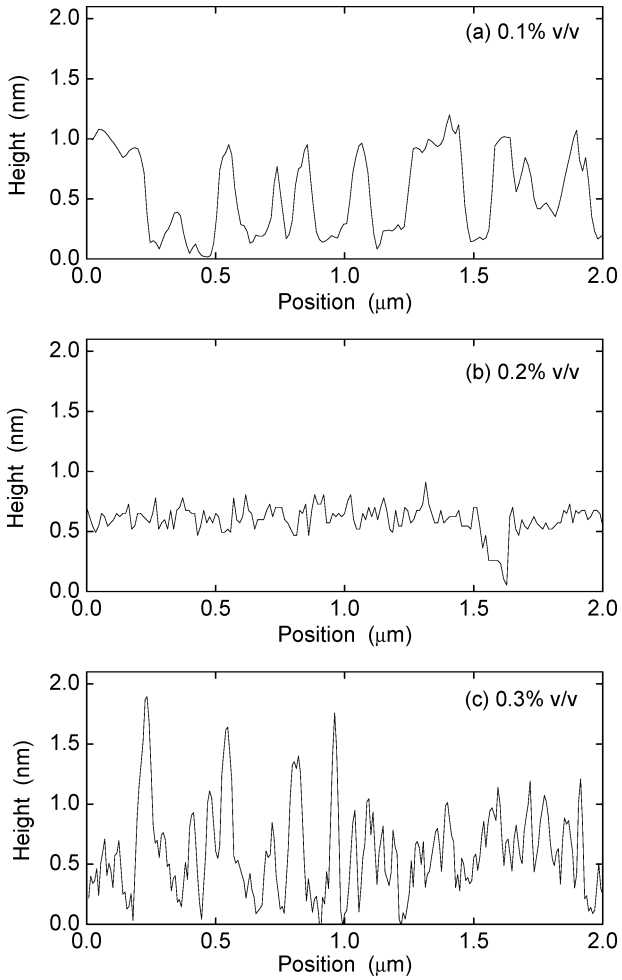

Figure 1. Height profile of phenyltrichlorosilane monolayers on mica, self-assembled at solution concentrations of (a) 0.1% v/v, (b) 0.2% v/v, and (c) 0.3% v/v. The profiles were measured with tapping mode AFM in air. The 0.2% v/v concentration was selected for the formation of all the monolayers on glass and mica used in the friction experiments.

linking to obtain a surface species with only Si−O bonds. Reference 18 gives molecular areas of 0.25 nm^2 for Ph and 0.35 nm^2 for Bz based on UV spectral data, whereas our ellipsometry results indicate that Bz is the more closely packed monolayer. The aromatic silanes can be compared to their thiol analogues, thiophenol (C_6H_5−SH) and benzyl mercaptan ($C_6H_5CH_2$−SH),[19] where it is known that the methyl group in benzyl mercaptan gives it enhanced rotational freedom[22,23] which leads to a much higher packing than thiophenol and a similar difference in contact angle hysteresis to the one we obtain for the silanes. This, taken together with the transition pressures obtained for the monolayers (cf. Figure 4b and 4d, and Table 3), suggests that Bz is indeed more closely packed than Ph.

Surface Forces Apparatus Friction Measurements. In the SFA,[24] normal forces and friction are measured between two macroscopic surfaces in a crossed-cylinder configuration which at small separations is equivalent to a sphere near a flat surface. The surfaces are micrometer-thin, transparent mica or glass sheets with silvered backsides, which form an optical interferometer that allows the determination of gap thickness[25,26] between the facing surfaces with an accuracy of 0.1−0.2 nm and contact diameter with an accuracy of 1−2 μm. The radius of the undeformed surfaces, R, can also be measured from the interference pattern. Compressive or tensile normal forces (load) are measured and regulated by moving the lower surface with mechanical stages and detecting the deflection of a double-cantilever leaf spring supporting it. In these experiments, performed at UC Santa Barbara, we used an "SFA3"[27] with sliding attachments as described in detail in ref 28.

In the SFA experiments, the surfaces were first brought into contact in dry N_2 gas and the wavelengths of the interference fringes noted. The thickness of the silane monolayers was obtained by comparing the interference wavelengths of monolayer-covered surfaces to the ones obtained with bare substrates in contact. This is easy to do in the case of mica substrates where several pairs with the same thickness can be prepared; but in the case of glass substrates, it requires removal of the monolayer by irradiation and remounting of the surfaces, which may introduce errors.[21] The glass substrates are always of different and nonuniform thickness so that the resulting interferometer is asymmetrical.[26]

To decrease the adhesion, a small droplet of ethanol (Gold Shield Chemical Co., "200 proof") was injected between the surfaces through a flush-cleaned Acrodisc CR PTFE syringe filter. Some ethanol was placed at the bottom of the instrument chamber to decrease the evaporation from the droplet. The friction was measured between two bare glass surfaces and with one or both glass surfaces covered with a silane monolayer. For comparison, experiments were also done with two mica surfaces covered with physiorbed Ph monolayers. All SFA measurements indicated that the thickness of chemisorbed Ph and Bz monolayers in dry N_2 or in ethanol was 0.8−0.9 nm (no change in monolayer thickness was observed upon adding ethanol), but in the case of physisorbed Ph layers on mica (cf. Figure 7 and discussion section), some changes from the initial 0.8−0.9 nm thickness could occasionally be seen after sliding in ethanol.

Friction forces were measured by sliding the lower surface laterally over a distance of 10−20 μm at a constant velocity (chosen in the range $v = 0.0004-0.5$ μm/s) with a piezoelectric "bimorph" sliding device and detecting the resulting deflection of cantilever springs holding the upper surface using four strain gauges ("full bridge" configuration). The strain gauge bridge is calibrated by measuring the deflection (with a traveling microscope) and output voltage when a known mass is placed on the springs. An example of the deflection or "friction trace" as a function of time during a friction experiment is shown in Figure 2a.

Friction Force Microscopy (FFM). The friction of the silane monolayers chemisorbed on glass was also measured with an atomic force microscope (Nanoscope III, Digital Instruments) at Åbo Akademi University. The FFM tips, listed in Table 2, were unfunctionalized Si tips assumed to have a native oxide layer (CSC12 and NSC12, MikroMasch, Tallinn, Estonia). A silane monolayer was deposited on tips 3 and 4 as described above. Scanning electron microscopy (SEM) was used to determine the thickness of the cantilevers and the height of the tips with an accuracy of 0.02 μm, as described in ref 19. The normal and lateral (torsional) spring constants given in Table 2 were calculated according to[3,29]

$$k_n = Ewh^3/(4L_c^3) \quad (2)$$

$$k_l = GK/(t^2L_c) \quad (3)$$

where E is Young's modulus and G the shear modulus of the cantilever material (Si),[3,29] $K = (wh^3/16)(16/3 - 3.36h/w)$, t is the tip height, w is the width, h is the thickness, and L_c is the length of the cantilever. On the basis of the accuracy of the SEM measurement, the spring constants would be determined

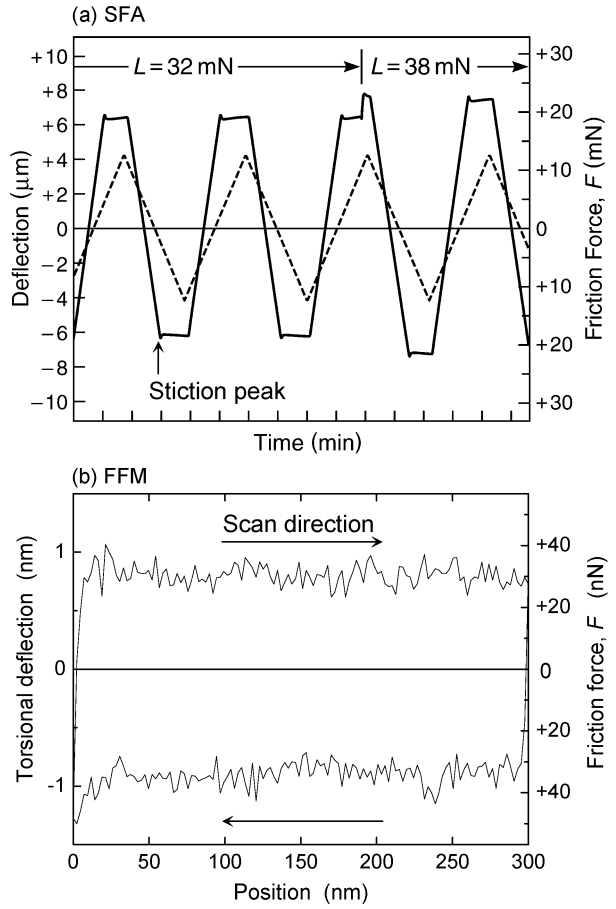

Figure 2. Examples of friction measurements with SFA and FFM. (a) SFA measurement of the friction between a bare glass surface and a phenyltrichlorosilane monolayer on glass in ethanol (solid curve). The sliding velocity was $v = 0.15$ μm/s, $R = 1.8$ cm, and L was 32 and 38 mN. A small "stiction peak" followed by smooth kinetic sliding was commonly seen when the sliding resumed after a change in the sliding direction, both for phenyltrichlorosilane and benzyltrichlorosilane sliding against glass and also in systems where both surfaces were covered with a monolayer. The dashed curve illustrates the lateral movement of the bimorph device (the lower surface) at a constant velocity (for clarity, its deflection is shown as 40% of the actual value). (b) FFM of phenyltrichlorosilane on glass in ethanol with unfunctionalized Si tip 2; sliding velocity $v = 3$ μm/s, $R = 33$ nm, $L = 99$ nN. The plot shows a "friction loop", i.e., torsional deflection as a function of sample position as the sample is scanned back and forth under the tip (perpendicularly to the cantilever beam).

with an accuracy of 3−7%. However, because the stiffness of the reflective aluminum layer on top of the beam was not taken into account in this calculation, the overall accuracy of k_n and k_l in Table 2 is 10−15%. The radius of each tip, R, was measured in two perpendicular directions by reverse imaging of a characterization grating consisting of sharp cones with an apex radius of curvature of <10 nm (model TGT01, Mikro-Masch, Estonia), and the geometric mean is given in Table 2.

The FFM experiments were done in a liquid cell filled with ethanol (Primalco, Finland, 99.5%) to reduce the interfacial energy between the glass surface or silane monolayers and the tips to $\gamma \leq 3$ mN/m.[9,10,30] Low adhesion leads to relatively small deformations and small contact areas at low loads, as predicted from the Johnson−Kendall−Roberts[31] (JKR) or DMT theories of contact mechanics.[32] For simplicity, the contact pressures have therefore been calculated assuming a Hertzian (nonadhesive) contact and an average elastic modulus $K_{eff} = (4/3)E^*$ for Si−glass or glass−glass. $E^* = [(1 - \nu_1^2)/E_1 + [(1 - \nu_2^2)/E_2]^{-1}$, where E_i is Young's modulus and ν_i Poisson's ratio for the materials. The maximum Hertzian pressure in the contact area is

$$P_0 = \frac{3}{2\pi}\left(\frac{K_{eff}}{R}\right)^{2/3} L^{1/3} = \frac{3L}{2A} \quad (4)$$

where A is the contact area.

The raw data in an FFM measurement consists of the deflection voltage (torsion of the cantilever) as a function of sample position (cf. Figure 2b). In a simple conversion from voltage to friction force, this signal is assumed to be only from torsion of the cantilever.[10,29,33−35] It is, however, influenced by deformation of the contact between the tip and sample (lateral contact stiffness)[2,33,35] and by bending of the outermost part of the tip itself.[36] For three of the cantilevers used in this study, the lateral (torsion) spring constants (Table 2) were at least an order of magnitude less than the ones discussed in refs 33 and 35.[19] In these cases, it is unlikely that tip bending or sample deformation contributes significantly to the sticking portion of the friction force trace of the raw data (used for conversion from voltage to deflection distance), which instead shows the torsion of the soft cantilever (cf. Figure 2b). However, for the stiffer cantilever (unfunctionalized Si tip 2) these effects may become important.[19] Slope calibration and conversion of this type should not be done for the silane-covered tips because of the low stiffness of the monolayer, but the conversion for tips 3 and 4 was assumed to be the same as for the unfunctionalized Si tip 1, which had similar dimensions and spring constants.

To obtain the large range of sliding velocities shown in Figures 3c and 6, friction data were taken over three different scan sizes (20, 300, and 750 nm) at frequencies of 0.02−61 Hz. The agreement between measurements at different scan size but the same sliding velocity was very good. The friction forces as a function of load in Figure 3b and Figure 4b and 4d were measured at 1 Hz over a scan size of 150 nm. The FFM experiments on bare glass substrates showed a more erratic sliding than on the monolayers, particularly at high loads, which is reflected in the larger error in the data in Figure 3b and 3c compared to Figures 4b, 4d, and 6.

An important difference between experiments with the SFA and FFM is the large difference in the contact area and pressure. The radius of curvature of the undeformed surfaces in our SFA experiments was $R = 0.2-2.8$ cm, whereas FFM tips typically have radii of 10−300 nm, depending on the type and manufacturing process. Within the load range that can be conveniently reached in the SFA, the *maximum* pressure in the contact area is generally less than 100 MPa, whereas the contact pressures in the FFM, even at low loads, are already several GPa.[4]

Results and Discussion

Strength of Adhesion in Ethanol. All adhesion and friction experiments were done in ethanol. No layering (oscillatory force) in ethanol[37] was detected with any of the FFM tips (unfunctionalized or monolayer-covered, $R = 11-33$ nm). Similarly, no layering of ethanol was observed in the SFA experiments, neither with bare nor with monolayer-covered glass surfaces ($R = 0.2-2.8$ cm). It is known that oscillatory forces do not appear in systems where the monolayers are loosely packed or consist of branched molecules because such surfaces are rough on a molecular scale which perturbs the layering of the confined liquid.[38] A comparison of the molecular areas in Table 1 to that expected on the basis of the covalent and van der Waals radii[23] of a vertically oriented benzene molecule, 0.21 nm^2, shows that neither of our silane monolayers is close-packed. The 0.2 nm

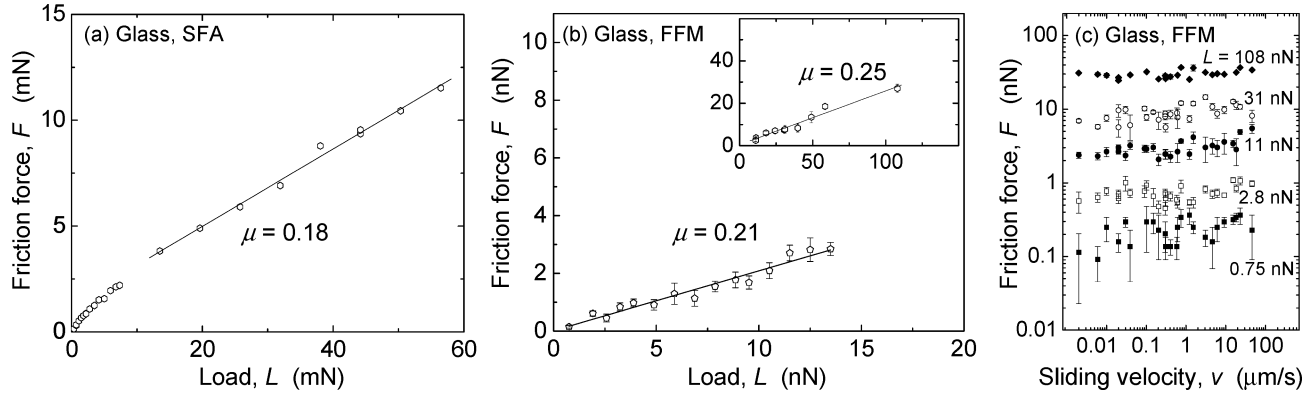

Figure 3. (a) Friction force vs load between two Pyrex glass surfaces ($R = 2.3$ cm) in ethanol, measured with the SFA at a sliding speed of 0.15 μm/s. The friction coefficient (fit to the linear part of the data) is $\mu = 0.18 \pm 0.01$. (b and c) FFM measurements in ethanol of a Pyrex glass surface sliding against two unfunctionalized Si tips of different radii and spring constants (tips 1 and 2 in Table 2). (b) Friction force vs load at a sliding speed of 0.15 μm/s. Main figure: tip 1, $R = 11$ nm, $\mu = 0.21 \pm 0.01$. Inset: tip 2, $R = 33$ nm, $\mu = 0.25 \pm 0.02$. (c) Friction force vs sliding velocity (scan speed) v at selected loads L. The data at $L = 0.75$ nN and $L = 2.8$ nN were measured with tip 1, and the higher loads were measured with tip 2. No velocity-dependence was observed.

rms roughness of the bare glass surface might also disturb the layering of the small ethanol molecules.[39]

Fitting the JKR equation for the dependence of the radius of the contact area, r, on the external load[31,32]

$$r^3 = \frac{R}{K_{\text{eff}}}[L + 6\pi R\gamma + \sqrt{12\pi R\gamma L + (6\pi R\gamma)^2}] \qquad (5)$$

to the measured values on loading in the SFA experiments gives interfacial energies below 1 mN/m for all combinations of monolayers and glass surfaces in ethanol except for glass−glass contact. At such low interfacial energies, the contact mechanics is not well-described by the JKR theory and the error is quite large, ±4 mN/m. Instead, our contact areas in these SFA experiments are well-described by the Hertz model, $r^3 = RL/K_{\text{eff}}$ (cf. Figure 5). The interfacial energy obtained from the JKR fit on loading in a glass−glass contact in ethanol (the system shown in Figure 3a) was slightly higher, $\gamma = 4 \pm 2$ mN/m. Because of plastic deformation of the UV glue after long times in contact (which changes R), it was not feasible to use unloading data to determine the interfacial energy. The low pull-off forces in the SFA experiments after short times in contact without an applied load gave $\gamma < 0.1$ mN/m.

In the FFM measurements, a weak adhesive minimum was seen below a distance of about 2 nm from the onset of strong repulsion (contact). The average adhesion force (pull-off force) on separation from this minimum, measured with unfunctionalized Si tips 1 and 2 and normalized by the measured tip radius, was $F_{\text{adh}}/R = -3$ to -17 mN/m. When the tip was covered with the corresponding thiol monolayer (tips 3 and 4), the adhesion force was $F_{\text{adh}}/R = -2$ to -24 mN/m. The interfacial energy γ in these systems is thus reduced by the presence of ethanol to $\gamma < 3$ mN/m (the range obtained from the F_{adh}/R values using a JKR or DMT model), as has been observed previously for CH_3-terminated alkanesilane and alkanethiol monolayers.[9,10]

The measured values of the adhesion force can be compared to the calculated van der Waals attraction between monolayers ($n = 1.53$, estimated thickness 0.7 nm) deposited on glass and adhering in ethanol ($n = 1.36$, $\epsilon = 25$). One finds that the calculated ethanol film thickness corresponding to the *measured* F_{adh}/R values was in most cases <0.3 nm between a monolayer or bare glass surface and Si tips 1 and 2 and <0.2 nm in contacts between a monolayer and the corresponding monolayer-covered tip 3 or 4. Because the average diameter of an ethanol molecule is 0.44 nm,[40] it is unlikely that a complete layer of ethanol is present between the surfaces even at low loads. Similar results have been obtained for aromatic thiol monolayers on gold.[19] In the SFA experiments it was found that the monolayer thickness in contact in dry N_2 and in ethanol was the same within the experimental error of 0.1−0.2 nm. One can therefore expect the friction response of these systems to arise mainly from the monolayers and not from a confined ethanol film. However, ethanol molecules may penetrate into the monolayers as will be discussed in connection with Figure 7.

Friction between Two Bare Glass Surfaces or Glass and Silicon Tips in Ethanol. Figure 3 shows the friction force between two bare glass surfaces (SFA, Figure 3a) and a glass surface and unfunctionalized Si tips (FFM, Figure 3b and 3c) in ethanol. Although occasional stick−slip-type sliding (regular slips with lengths of 200−400 nm, depending on the load) was seen at low loads in some SFA experiments on bare glass, the data in Figure 3a were obtained in the more typical situation of smooth sliding (kinetic friction only), that is, similar to that shown for glass against a silane monolayer in Figure 2a but without a stiction peak. Occasional large peaks, suggesting slips with a length of 3−4 nm, were also seen in the FFM "friction loops" obtained in Si-on-glass sliding in ethanol at low loads. Note the different scales (mN in Figure 3a and nN in Figure 3b and 3c).

There is good agreement between the friction coefficients obtained with the two techniques for these similar systems. A recent study of the friction between two gold surfaces and between two aromatic thiol monolayers under conditions of low adhesion ($\gamma = 1-4$ mN/m) showed a similar agreement for the friction coefficients obtained with FFM tips of very different radii.[19] Evidently, this conclusion can now be extended to experiments with the SFA where R is 5−6 orders of magnitude larger.

In contrast to the rest of the data in this study, the friction force as a function of load measured between the bare glass surfaces with the SFA was not completely linear at the lowest loads (Figure 3a) even though the friction force goes to zero at zero load. This correlates with the slightly larger interfacial energy ($\gamma = 4 \pm 2$ mN/m) measured for the glass−glass contact in ethanol. However, the range of γ investigated here was too limited to establish a value below which only an apparently linear dependence on the load arises.

FFM measurements with unfunctionalized Si tips 1 and 2 against a bare glass surface in ethanol showed that the friction

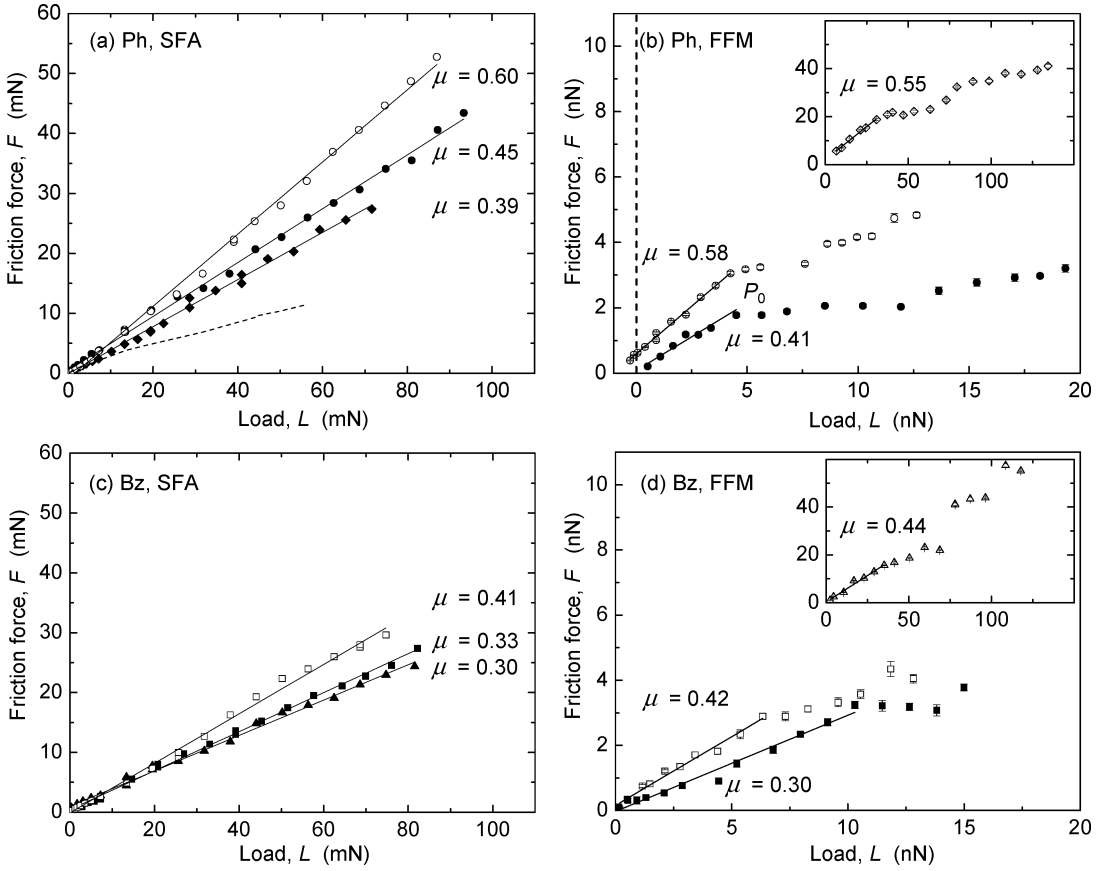

Figure 4. Load-dependence of the friction forces of monolayers of phenyltrichlorosilane (Ph) and benzyltrichlorosilane (Bz) monolayers in ethanol measured with the SFA at sliding velocities of $v = 0.5$ μm/s (open and solid circles and squares in panels a and c) and $v = 0.15$ μm/s (solid diamonds and triangles in panels a and c) and with the FFM at $v = 0.15$ μm/s (panels b and d). Open symbols denote sliding of a monolayer on glass against a bare Pyrex glass surface in the SFA or unfunctionalized Si (tips 1 and 2, Table 2) in the FFM experiments. Filled symbols show results from systems with both surfaces covered with the respective silane monolayer (using tips 3 and 4 in panels b and d, respectively). The insets in panels b and d show FFM data obtained with tip 2, which was stiffer than the other cantilevers. The friction coefficients, μ, and the maximum pressures, P_0, at the onset of each plateau in the FFM data are listed in Table 3. The dashed curve in panel a is the friction force between two bare glass surfaces in ethanol (from Figure 3a).

force in this system had no distinct velocity-dependence over a wide range of velocities and loads (Figure 3c).

Friction of Self-Assembled Monolayers in Ethanol. Figure 4 shows the friction force as a function of load measured with both techniques in systems where one or both of the sliding surfaces is covered with a chemically bound Ph or Bz monolayer (cf. Table 1). As for the case of bare glass substrates or Si sliding on glass in ethanol (Figure 3), very different contact areas and loads still give a linear dependence of F on L with the same friction coefficient for comparable systems, and again $F \rightarrow 0$ as $L \rightarrow 0$ (except for one case in Figure 4b). In additional SFA experiments on Ph, similar friction coefficients were obtained also at sliding velocities of 0.004−0.016 μm/s (not shown), which agrees well with the weak velocity-dependence of these systems measured with FFM (Figure 6). The friction decreased when both sliding surfaces were covered with a monolayer (filled symbols).

Figure 5 shows the contact areas measured in three of the SFA experiments in Figure 4a and 4c. In all cases, the contact area as a function of load was well-described by the Hertz model. In some experiments, a fairly thick glue layer was needed to accommodate the inherent curvature of the glass sheets, and the resulting effective elastic modulus K_{eff} was quite low, 7×10^7 to 2×10^9 N/m^2. In experiments using mica sheets (Figure 7), thinner glue layers were used and K_{eff} was 1×10^9 to 2×10^{10} N/m^2, which is within the typical range found in SFA experiments using mica, also in experiments using other types of glues.[41]

In the FFM measurements (Figure 4b and 4d), the plateaus in the data at higher loads suggest transitions in the monolayers, similar to previous observations on alkanethiol[42,43] and aromatic thiol monolayers on gold.[19] In contrast to the thiol-on-gold systems, where the lattice structure of the gold appears in the AFM images at high loads, images obtained both above and below the plateau in our silane systems are featureless and give no indication of the nature of the transition. Table 3 shows the values obtained from Figure 4 for the friction coefficients μ and the maximum pressures at the onset of the plateaus P_0, together with the measured radii of the undeformed surfaces R. The transition occurs at higher pressure for Bz and is not dependent on whether the system contains one or two monolayers. As described in the Materials and Methods, the pressure in the contact region in the SFA is much lower than in the FFM, and no transitions in the friction forces or in the thicknesses of the confined layers where observed in the SFA experiments.

The P_0 values obtained from Figure 4b and 4d can be compared to values for the corresponding aromatic thiol monolayers on gold.[19] Alkylsilanes are known to form more irregular and loose-packed monolayers than are formed by the corresponding alkanethiols because of the cross-linking and the different density of sites on the substrate,[7,10,44] and this is also seen for aromatic systems: For benzyl mercaptan monolayers

TABLE 3: Radii of the Undeformed Surfaces *R*, Friction Coefficients μ in Ethanol at Low Loads, and Maximum Pressure P_0 at the Onset of the Plateau in the *F* vs *L* Curves (Figure 4)

	Si tip or glass/Ph			Si tip or glass/Bz			Ph/Ph			Bz/Bz		
	R (m)	μ	P_0 (GPa)	R (m)	μ	P_0 (GPa)	R (m)	μ	P_0 (GPa)	R (m)	μ	P_0 (GPa)
SFA[a]	1.1×10^{-2}	0.60 ± 0.01		1.5×10^{-2}	0.41 ± 0.01		0.9×10^{-2}	0.45 ± 0.01		0.8×10^{-2}	0.33 ± 0.01	
							0.5×10^{-2}	0.39 ± 0.01		2.6×10^{-2}	0.30 ± 0.01	
FFM[b]	11×10^{-9}	0.58 ± 0.01	2.2	11×10^{-9}	0.42 ± 0.02	2.6	16×10^{-9}	0.41 ± 0.05	2.1	11×10^{-9}	0.30 ± 0.01	2.7
	33×10^{-9}	0.55 ± 0.02	2.3	33×10^{-9}	0.44 ± 0.02	2.5						

[a] SFA experiments were done with one or both glass surfaces covered with a monolayer. The first row of SFA data was obtained at $v = 0.5$ μm/s and the second at $v = 0.15$ μm/s. [b] FFM data were obtained with bare and monolayer-covered Si tips 1−4 (cf. Table 2) at $v = 0.15$ μm/s.

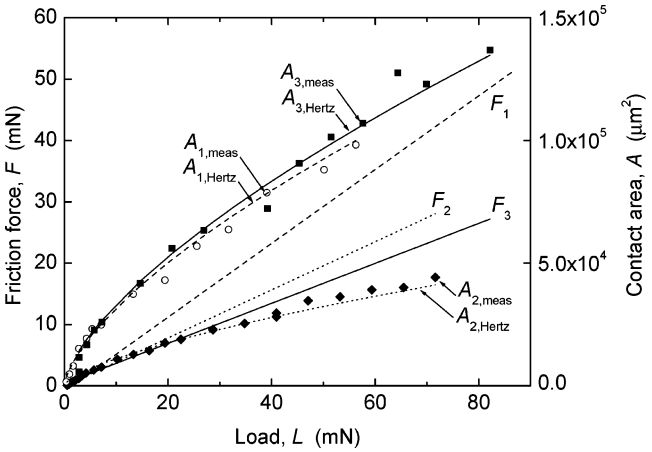

Figure 5. Contact areas and friction forces in three of the SFA experiments shown in Figure 4a and 4c. F_1 is the friction force between bare glass and a Ph monolayer ($\mu = 0.60$ in Figure 4a, shown here as a dashed straight line), $A_{1,meas}$ (open circles) is the experimentally measured area, and $A_{1,Hertz}$ (dashed curve) is a Hertzian fit ($R = 1.1$ cm, $K_{eff} = 1.1 \times 10^8$ N/m^2). F_2 (dotted straight line, $\mu = 0.39$) is the friction force between two Ph monolayers at $v = 0.15$ μm/s, with $A_{2,meas}$ (diamonds) and $A_{2,Hertz}$ (dotted curve, $R = 0.5$ cm, $K_{eff} = 2.3 \times 10^8$ N/m^2). F_3 (solid straight line, $\mu = 0.33$) is the friction force between two Bz monolayers at $v = 0.5$ μm/s, with $A_{3,meas}$ (squares) and $A_{3,Hertz}$ (solid curve, $R = 0.8$ cm, $K_{eff} = 7.4 \times 10^7$ N/m^2).

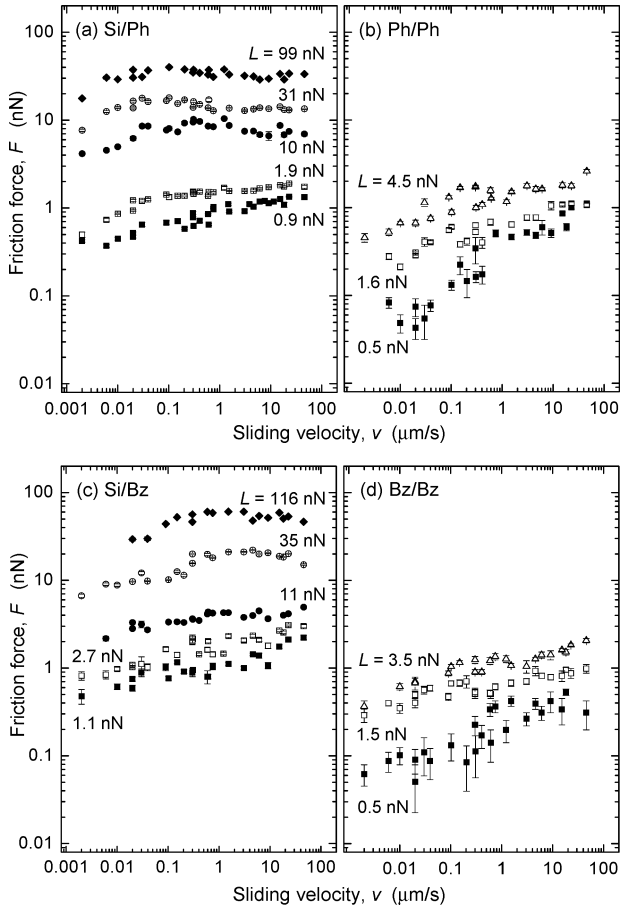

Figure 6. Velocity-dependence of the friction force between aromatic silane monolayers in ethanol at selected loads: (a) Ph monolayer on glass against unfunctionalized Si tip 1 (two lowest loads, $L = 0.9$ nN and $L = 1.9$ nN) and tip 2 (three higher loads); (b) Ph monolayer on glass against Ph-covered tip 3; (c) Bz monolayer on glass against unfunctionalized Si tips 1 and 2; (d) Bz monolayer on glass against Bz-covered tip 4.

($C_6H_5CH_2-SH$, molecular area 0.20 nm^2) the transition starts at $P_0 = 2.6-3.2$ GPa,[19] and for Bz (molecular area 0.27 nm^2) the transition starts at 2.5−2.7 GPa (Table 3). For a more loose-packed monolayer such as thiophenol (C_6H_5-SH, molecular area ca. 0.35 nm^2) the transition occurs[19] at 2.3−2.6 GPa, and for Ph (molecular area 0.45 nm^2) the transition occurs at 2.1−2.3 GPa. Although the friction coefficients after the plateaus in Figure 4b and 4d become similar for all systems and approach the one for bare glass in ethanol, the observation of a transition does not necessarily imply that the monolayer is removed from the contact, because the linear regime of the friction force at low loads was recovered on decreasing the load, as for the aromatic thiol monolayers.[19]

Velocity-Dependence of Monolayer Friction. The friction of chemisorbed SAMs measured with the SFA did not show a strong velocity-dependence in the range of velocities investigated, $v = 0.004-0.5$ μm/s. Figure 6 shows the velocity-dependence of the friction of the monolayers measured with FFM. In the cases where the monolayers were sliding against an unfunctionalized tip (Figure 6a and 6c), there was either no distinct velocity-dependence or only a slight increase in the friction force with v. Similar results have been obtained for loose-packed thiophenol monolayers on gold.[19] At high loads ($L = 35$ nN and $L = 116$ nN), a maximum or different, higher plateau appears in the Si/Bz data (Figure 6c) around $v = 0.5$ μm/s. This is indicative of a more rigid response of this more closely packed silane monolayer, appearing only at the higher loads. In even more close-packed aromatic thiol monolayers (aminothiophenol and benzyl mercaptan) such a maximum or plateau appeared already at low loads[19] and was shifted toward lower velocity with increasing load. The appearance of the higher plateau in the Bz friction in this load and velocity-range correlates well with the calculated packing of the Bz monolayer, showing it to be intermediate between that of benzyl mercaptan and thiophenol on gold.

When both surfaces carry monolayers (Figure 6b and 6d), the investigated loads are apparently too low to induce any clear maximum or plateau in the data for either system. Instead, the lower friction than at similar loads in Figure 6a and 6c and the continuous increase with velocity suggest a more fluid-like film than is found with only one monolayer in the contact; that is, any possible maxima or plateaus would be at higher sliding

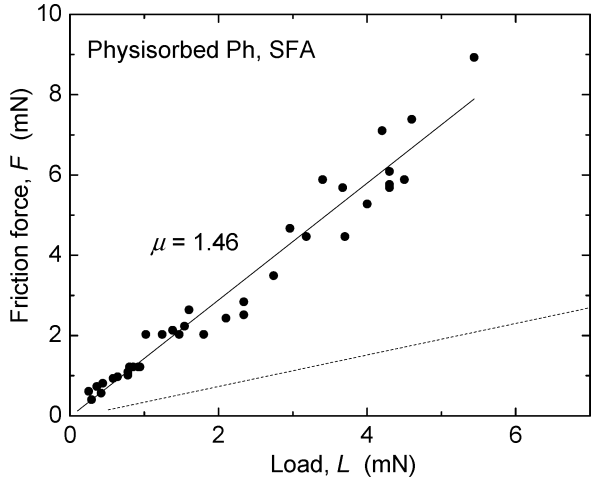

Figure 7. Load-dependence of the friction force between two physisorbed phenyltrichlorosilane monolayers on mica surfaces ($R = 0.8-2.8$ cm) measured in ethanol with the SFA at sliding velocities of $v = 0.0008-0.004$ μm/s. The friction coefficient was very high, $\mu = 1.46 \pm 0.05$. Higher sliding velocities or higher loads led to damage of the surfaces. The dotted line shows the friction force measured between two chemisorbed phenyltrichlorosilane monolayers on glass at $v = 0.15$ μm/s (data shown as filled diamonds in Figure 4a, $\mu = 0.39$), where it was possible to go to much higher loads and sliding speeds without damaging the surfaces.

velocities and loads than the ones investigated in Figure 6b and 6d. Compared to aromatic thiols, the aromatic silane monolayers are too loose-packed and irregular to give different velocity responses in the regime investigated, but they show an overall lower friction, even in systems with only one surface covered with a monolayer.

Physisorbed Phenyltrichlorosilane Monolayer. Trichlorosilane monolayers can be formed on mica according to the same procedure as is used on glass and Si (cf. Materials and Methods). Because the mica surface does not expose reactive groups, the laterally cross-linked monolayer is only *physisorbed* to the substrate. In a solvent, such monolayers are very easily removed or damaged during sliding because of solvent penetration which weakens the adhesion of the monolayer to the substrate. Figure 7 shows data from six different SFA experiments in ethanol where both mica surfaces were covered with a phenyltrichlorosilane monolayer. Fits of the JKR equation (eq 5) to the radius of the contact area on loading gave $\gamma = 1 \pm 2$ mN/m. This system also shows a linear dependence of the friction force on load but with a much higher friction coefficient than when glass was used as the substrate (dotted line in Figure 7). The low contact angle of water on these monolayers (Table 1) indicates that the monolayers are not as well-formed on mica as on glass, although the confined total film thickness, 1.6−1.9 nm, suggests a Ph monolayer thickness of 0.8−0.9 nm.

During sliding, ethanol penetrates into and under the physisorbed monolayers and causes the formation of a different confined film with a total thickness of about 3.5−4 nm and a friction coefficient of about 0.8 (not shown). Similarly to the original monolayers (thickness 0.8−0.9 nm, Figure 7), this thicker film did not protect the mica surfaces from wear at loads above about 5 mN. In contrast, the Ph and Bz monolayers on glass generally protected the glass surface from wear even at the highest loads used in Figure 4a and 4c, and no changes were seen in the confined film thickness.

Contact Angle Measurements: Correlation with Friction Forces. Contact angle measurements provide information about the chemistry and homogeneity of a surface. Even in cases where different monolayers expose the same functional group to the monolayer/air interface (as in the case of our aromatic silanes), monolayer molecules that are loosely packed or only physisorbed to a surface may rearrange or even turn over when in contact with water to give a larger contact angle hysteresis than close-packed or chemically bound ones. Contact angle hysteresis is associated with other energy-dissipating processes such as adhesion hysteresis and friction.[1] The relative magnitude of the friction of Ph and Bz correlates with their contact angle hysteresis ($\cos\theta_{rec} - \cos\theta_{adv}$, cf. Table 1), which also correlates with their molecular areas on Si(111). Comparison with aromatic thiol monolayers[19] shows that in systems where both surfaces are covered with a monolayer, a higher friction is obtained for the more loosely packed thiophenol than for benzyl mercaptan. Thiophenol and benzyl mercaptan monolayers on gold give higher contact angles than the silane monolayers on glass but very similar contact angle hysteresis ($\cos\theta_{rec} - \cos\theta_{adv} \approx 0.45 \pm 0.05$ and 0.28 ± 0.05, respectively).

Conclusions

We have studied the friction of aromatic silane monolayers with SFA and FFM in systems with low adhesion ($\gamma < 3$ mN/m). For these conditions, the friction was linearly proportional to the external load even at low loads, and we found good agreement between the friction coefficients obtained with these two techniques despite the very large differences in contact area, load, and pressure. This is in contrast to results obtained for confined polymer films,[4] where different pressures can lead to different film thicknesses and intrinsic friction forces. It is also different from adhesive systems, where the friction force is typically proportional to the contact area at low loads.[1,2,5,6] Work is currently underway to compare the experimentally observed differences between adhesive and nonadhesive systems with molecular dynamics simulations carried out by Landman and co-workers.[45] The different friction responses of the silane monolayers correlate well with their contact angle hysteresis and molecular area. Lower friction was found in systems where both sliding surfaces are covered with a monolayer, and chemically bound monolayers showed a much higher stability to wear than physisorbed layers.

Acknowledgment. We thank A. Parra, C. Ekholm, B. Westman, and M. Csuja for technical assistance. The trichlorosilanes were obtained with the efficient help of J. Kramer at ABCR GmbH. M.R. thanks the Academy of Finland (Grant No. 48879), Åbo Akademi University, the Ella and Georg Ehrnrooth Foundation, the Research Institute at Åbo Akademi, and the Magnus Ehrnrooth Foundation for financial support. This work was supported by ONR Grant No. N00014-00-1-0214 and made use of MRL Central Facilities supported by the MRSEC Program of the NSF under Award No. DMR00-80034.

References and Notes

(1) Israelachvili, J. N.; Berman, A. D. In *Handbook of Micro/Nanotribology*, 2nd ed.; Bhushan, B., Ed.; CRC Press: Boca Raton, FL, 1999; pp 371−432.

(2) Carpick, R. W.; Salmeron, M. *Chem. Rev.* **1997**, *97*, 1163.

(3) Meyer, E.; Overney, R. M.; Dransfeldt, K.; Gyalog, T. *Nanoscience: Friction and Rheology on the Nanometer Scale*; World Scientific: Singapore, 1998.

(4) McGuiggan, P. M.; Zhang, J.; Hsu, S. M. *Tribol. Lett.* **2001**, *10*, 217.

(5) Enachescu, M.; van den Oetelaar, R. J. A.; Carpick, R. W.; Ogletree, D. F.; Flipse, C. F. J.; Salmeron, M. *Tribol. Lett.* **1999**, *7*, 73.

(6) Kim, H. I.; Houston, J. E. *J. Am. Chem. Soc.* **2000**, *112*, 12045.

(7) Lio, A.; Charych, D. H.; Salmeron, M. *J. Phys. Chem. B* **1997**, *101*, 3800.
(8) Schwarz, U. D.; Allers, W.; Gensterblum, G.; Wiesendanger, R. *Phys. Rev. B* **1995**, *52*, 14976.
(9) Noy, A.; Frisbie, D.; Rozsnyai, L. F.; Wrighton, M. S.; Lieber, C. M. *J. Am. Chem. Soc.* **1995**, *117*, 7943.
(10) Clear, S. C.; Nealey, P. F. *J. Colloid Interface Sci.* **1999**, *213*, 238.
(11) Li, L.; Yu, Q.; Jiang, S. *J. Phys. Chem. B* **1999**, *103*, 8290.
(12) Berman, A.; Drummond, C.; Israelachvili, J. *Tribol. Lett.* **1998**, *4*, 95.
(13) Briscoe, B. J.; Evans, D. C. B. *Proc. R. Soc. London, Ser. A* **1982**, *380*, 389.
(14) Derjaguin, B. V. *Z. Phys.* **1934**, *88*, 661. Derjaguin, B. V. *Wear* **1988**, *128*, 19.
(15) A third contribution to friction arises in lubricated sliding from the viscous drag force, $F = \eta A v/D$, where η is the viscosity, v is the sliding velocity, and D is the gap or film thickness. For Newtonian liquids (i.e., constant η, implying low L, $D > 1-10$ nm) F is proportional to A at constant v and D; but in practice both D and η usually depend on L.
(16) Heenan, D. F.; Januszkiewicz, K. R.; Sulek, H. H. *Wear* **1988**, *123*, 257.
(17) Dulcey, C. S.; Georger, J. H., Jr.; Krauthammer, V.; Stenger, D. A.; Fare, T. L.; Calvert, J. M. *Science* **1991**, *252*, 551.
(18) Dulcey, C. S.; Georger, J. H.; Chen, M.-S.; McElvany, S. W.; O'Ferrall, C. E.; Benezra, V. I.; Calvert, J. M. *Langmuir* **1996**, *12*, 1638.
(19) Ruths, M. *Langmuir* **2003**, *19*, 6788.
(20) Horn, R. G.; Smith, D. T.; Haller, W. *Chem. Phys. Lett.* **1989**, *162*, 404.
(21) Ruths, M.; Johannsmann, D.; Rühe, J.; Knoll, W. *Macromolecules* **2000**, *33*, 3860.
(22) Tao, Y.-T.; Wu, C.-C.; Eu, J.-Y.; Lin, W.-L.; Wu, K.-C.; Chen, C.-h. *Langmuir* **1997**, *13*, 4018.
(23) Jung, H. H.; Won, Y. D.; Shin, S.; Kim, K. *Langmuir* **1999**, *15*, 1147.
(24) Israelachvili, J. N.; Adams, G. E. *J. Chem. Soc., Faraday Trans. 1* **1978**, *74*, 975.
(25) Israelachvili, J. N. *J. Colloid Interface Sci.* **1973**, *44*, 259.
(26) Horn, R. G.; Smith, D. T. *Appl. Opt.* **1991**, *30*, 59.
(27) Israelachvili, J. N.; McGuiggan, P. M. *J. Mater. Res.* **1990**, *5*, 2223.
(28) Luengo, G.; Schmitt, F.-J.; Hill, R.; Israelachvili, J. *Macromolecules* **1997**, *30*, 2482.
(29) Liu, Y.; Wu, T.; Evans, D. F. *Langmuir* **1994**, *10*, 2241. Liu, Y.; Evans, D. F.; Song, Q.; Grainger, D. W. *Langmuir* **1996**, *12*, 1235.
(30) Weisenhorn, A. L.; Maivald, P.; Butt, H.-J.; Hansma, P. K. *Phys. Rev. B* **1992**, *45*, 11226.
(31) Johnson, K. L.; Kendall, K.; Roberts, A. D. *Proc. R. Soc. London, Ser. A* **1971**, *324*, 301.
(32) Israelachvili, J. N. *Intermolecular and Surface Forces*, 2nd ed.; Academic Press: London, 1991.
(33) Carpick, R. W.; Ogletree, D. F.; Salmeron, M. *Appl. Phys. Lett.* **1997**, *70*, 1548.
(34) Cain, R. G.; Reitsma, M. G.; Biggs, S.; Page, N. W. *Rev. Sci. Instrum.* **2001**, *72*, 3304.
(35) Piétrement, O.; Beaudoin, J. L.; Troyon, M. *Tribol. Lett.* **1999**, *7*, 213.
(36) Lantz, M. A.; O'Shea, S. J.; Hoole, A. C. F.; Welland, M. E. *Appl. Phys. Lett.* **1997**, *70*, 970.
(37) Wanless, E. J.; Christenson, H. K. *J. Chem. Phys.* **1994**, *101*, 4260.
(38) Gee, M. L.; Israelachvili, J. N. *J. Chem. Soc., Faraday Trans.* **1990**, *86*, 4049.
(39) Frink, L. J. D.; van Swol, F. *J. Chem. Phys.* **1998**, *108*, 5588.
(40) Löning, S.; Horst, C.; Hoffmann, U. *Chem. Eng. Technol.* **2001**, *24*, 242.
(41) Christenson, H. K. *Langmuir* **1996**, *12*, 1404.
(42) Liu, G.-y.; Salmeron, M. B. *Langmuir* **1994**, *10*, 367.
(43) Lio, A.; Morant, C.; Ogletree, D. F.; Salmeron, M. *J. Phys. Chem. B* **1997**, *101*, 4767.
(44) Ulman, A. *An Introduction to Ultrathin Organic Films*; Academic Press: Boston, MA, 1991.
(45) Gao, J.; Luedtke, W. D.; Landman, U. Georgia Institute of Technology. Personal communication, 2003.